Status of the Shielding Design of the SNS Accelerator System

Franz X. Gallmeier and Irina I. Popova

Oak Ridge National Laboratory
P.O. Box 2008, MS6474
Oak Ridge, Tennessee 37830, USA
gallmeierfz@ornl.gov

Abstract - *As the construction of the SNS Accelerator tunnel approaches completion, and commissioning of the ion source and front end systems are started, the demand of characterizing the radiation environment, and configuring shielding has not come to a halt yet. Detailed shielding analyses were performed along the entire accelerator line to identify high radiation areas, which are the injection, collimator and extraction sections of the accumulator ring, with special interest in the evaluation of the earth-berm as a primary radiation shield. Furthermore, design changes required a re-analysis of different accelerator sections during normal operation:*

- *The labyrinth in the front end building was designed to protect people working near the ion source;*
- *The doors for shielding the truck access ways to the accelerator tunnel were configured;*
- *Worst cases of accident scenarios of full beam losses in the linac-to-accumulator ring and the accumulator ring-to-target transfer lines were investigated;*
- *The energy deposition to the beam dumps due to changes in the incident beam profiles and the location of beam windows were recalculated;*
- *Water activation in the linac systems and in the collimators was performed.*

An update to the whole body of analyses will be given.

I. INTRODUCTION

At Oak Ridge National Laboratory a Spallation Neutron Source (SNS)[1] is in construction, which will become a world class neutron scattering facility. A high current beam of 1 GeV protons generated in a linac[2] will direct 1.4 MW power on to a liquid mercury target for production of high intense neutron beams. The radiation fields due to controlled and uncontrolled beam losses in the accelerator structures are mitigated by sufficient shielding. On the other side, we were searching for solutions as lean as possible for cost reasons. Also the activation of components and media was forecasted for planning of maintenance and waste streams. Much of the work is already published in previous proceedings of this series and elsewhere[3-8], however, we felt an update of the neutronics work on the SNS accelerator systems would be appreciated, and was tried here.

II. FRONT END SHIELDING DESIGN

The operational proton losses appear along the accelerator beam line in the SNS LINAC, which consists of a drift tube linac (DTL) section, a coupled cavity linac (CCL) section and a super conducting linac (SCL) section[2]. The very first 10 meters of the LINAC, the first and second DTL tank, are moved back into the front-end building where they connect to the ion source. Hence, the linac tunnel is extended back by permanent shielding to form a cave that surrounds these 10 meters of DTL structures (see Fig. 1). For personnel access an access way is being built leading to an opening in the north shielding wall. For feeding cable trays and wave guides into the cave from the adjacent klystron building, four openings are cut in the south shielding wall. These openings allow the propagation of radiation to the area outside the permanent shielding walls. Analyses were required for the evaluating the dose rates around the penetrations and for configuring and optimizing a shielding labyrinth for the access way.

At the time of the study, it was not clear as to how much space will be available for shielding at the back end of the cave. Hence no shielding was considered there. Also the x-ray sources from dark currents caused by radio frequency fields in the linac structures were not considered.

Transport analyses were performed with the MCNPX[9] code modeling the H^- beam loss[10] at 2.1 mA beam current according to the SNS beam loss document[10]

and the buildup of the secondary radiation field in the tunnel and front end building. Dose rate estimates were taken with surface flux type tallies and with mesh tallies. The beam losses were considered throughout the DTL of about 36 meters length to include also the backstreaming through the tunnel form further downstream linac sections. For the labyrinth design, calculations for a number of shielding configuration and material variations and were performed to find the optimal design.

The front-end model includes the front-end building with permanent shielding around the DTL tanks inside the building and the DTL part of the linac including the tunnel structure. The model of the DTL tanks was taken from previous studies[6] and combined with the front-end building geometry model. This includes the first DTL tank, partially the second DTL tank, the permanent 0.9-meter-thick shielding walls and the cave ceiling of 0.6 meter thickness around the DTL tanks. The shielding labyrinth for the access way at the north side of the DTL provides a 1.2-meters-wide walkway around 0.9 meter thick and 2.7-meters-high columns. A 0.6-meter-thick ceiling extends from the access opening in the cave wall over the first column to the second column. A 0.6-meter-thick and 2.7-meters-high shielding extends at the inside of the front-end building north wall from the front wall to the second labyrinth column, and is followed by a 0.3-meter-thick shielding to the outer end of the third column. The north wall itself is actually hollow and does not provide any neutron/gamma shielding. It is a sandwich of two thin steel sheets with low density filling for thermal insulation. The south cave wall is penetrated by four openings for wave guides and cable trays directed to the klystron building, which attaches to the front-end building on the south side. They lie at an elevation about 2.7 meters from the floor and are 0.9 meters high. The front-end building south wall is from concrete. The front-end building is a two story construction forming a base level and a mezzanine level covered by thin sheet metal roof. The mezzanine floor is 0.1 meters thick.

The recommended design of labyrinth settled after several iterations on the configuration using three columns. Ordinary concrete was used for the columns, but borated concrete for the north wall shielding. A reduction of the column thickness from 0.9 to 0.6 meters can be tolerated. Extending the labyrinth ceiling to the second column was required to reduce the dose levels outside of the north wall to below 0.25 mrem/hr. A horizontal dose rate map of the labyrinth is presented in Fig. 2. On the south cave wall, the dose rates at the openings were estimated ranging from 6 mrem/hr for the most upstream to 88 mrem/hr for the most downstream location. Personnel working in this area will be exposed up to 5 mrem/hr. This recommends the area for restricted access only. Similarly, the dose rate levels of 1.5 mrem/hr on the mezzanine are slightly above the design goal.

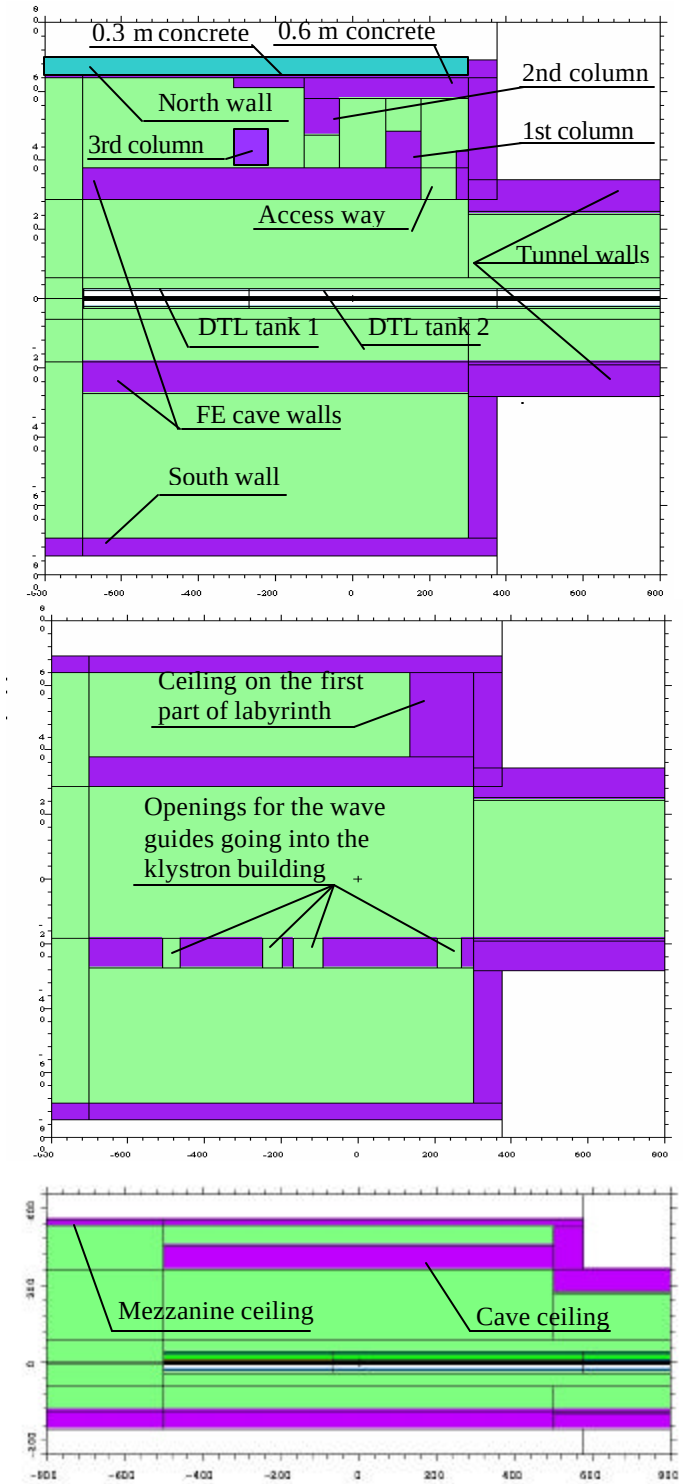

Fig. 1: Frontend building geometry: from top to bottom, horizontal cuts at beam level, at 2.4 m from floor level, and vertical cut through beam level.

III. TRUCK ACCESS DESIGN

During normal operation, proton losses appear along the beam in the SNS accelerator tunnel, and produce a radiation field that is safely shielded by a sufficiently thick earth-berm. Out of necessity there are penetration in the bulk shielding among the largest among them are two truck accesses. The first access is adjacent to the first straight section of the linac-to-ring beam transfer line and is wider and shorter than the second one, which is adjacent to the ring-to-target beam transfer line. Both truck accesses are designed as straight tunnels leading from the accelerator tunnel directly to the outside. They need to be properly closed with adequate amount of shielding blocks or with door during operation in order to maintain the radiation level outside of the accelerator tunnel below 0.25 mrem/h for unlimited access by a non-radiological worker as given by the 10CFR-835 US-DOE guideline.

Analyses were performed to optimize the truck access doors in the linac-to-ring beam transfer line, the results of which are presented here. Calculations for the ring-to-target truck access are still outstanding. A full blown model of the tunnel system and accelerator components was built including the straight beam transfer line connecting to the linac, and the 90 degree turn towards the accumulator ring as demonstrated in Fig. 3.

Controlled and uncontrolled loss terms [10] are modeled in MCNPX reflecting a fraction of 10^{-5} of the beam lost in the collimators left of the truck access, and a fraction of 10^{-3} of the beam lost in the beam stop in the arc to the right of the truck access, overlaid over a generic beam loss of 1W/meter. Analyses were performed in steps by producing surface sources in cross sections of the truck access tunnels at the entrance and at the truck access door. This problem was picked up benchmark case comparing different methodologies of shielding analyses[11].

At the entrance of the truck access dose rates of about 60 Rem/hr are expected during operation, which drop to about 3 Rem/hr in front of the truck access door. The dose attenuation in the door is plotted in Fig. 4. The optimization settled on a door consisting of 1.35 meters of scrape metal steel followed by 0.45 meters of concrete. An overlap of the door of 1.55 meters is recommended 0.25 meters of which must be from steel. Increasing the steel overlap might reduce the total overlap needed.

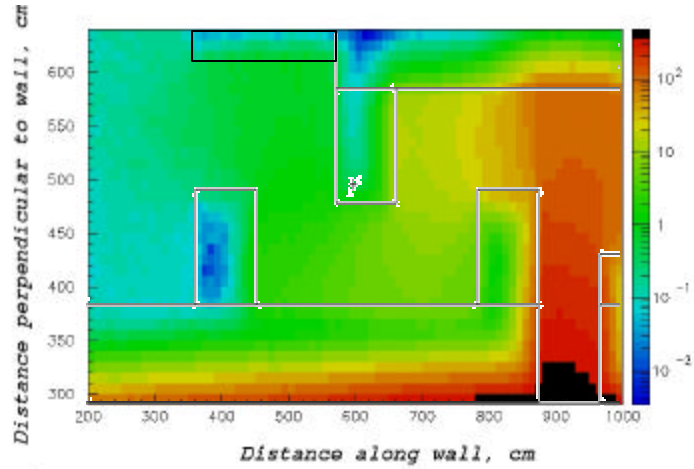

Fig. 2: Map of dose rates in the labyrinth of the access way to the north of the DTL shielding cave.

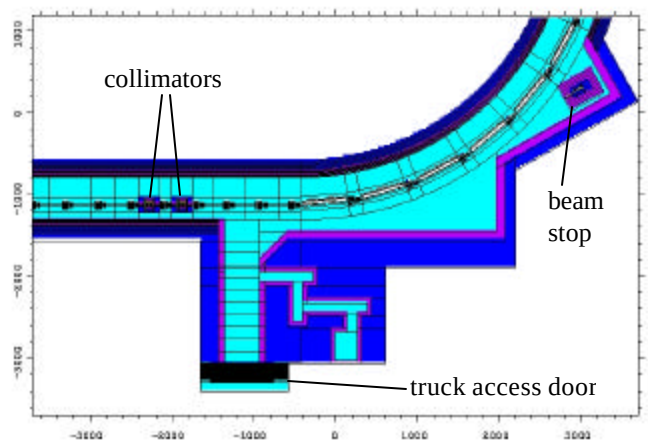

Fig. 3: MCNPX model of linac-to-ring beam transfer line including truck access.

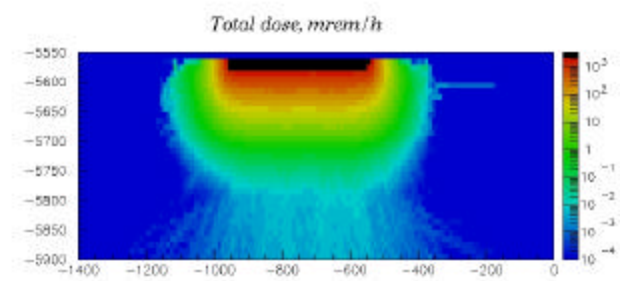

Fig. 4: A map of dose rates through a cross section cut of the truck access door of 1.35 m scrape metal steel and 0.5 m concrete.

IV. WORST CASE ACCIDENT SCENARIOS

The worst accident in the SNS accelerator system was considered to be a loss of the full 2MW 1GeV proton beam. In most accident scenarios, the lost beam is spread over a large tunnel section. Radiation monitors in the tunnel will pick up the accident, trigger the machine/personal protection system, and shut the beam off within 2 pulses/2 seconds. In one very unlikely but possible scenario the first linac-to-ring dipole is operating and bends the beam about 11 degrees with regard to the linac axis, whereas all the following dipoles fail. In this case the beam would go straight into the second dipole, will exit the bent beam pipe, leak out through the open dipole side, and will run more or less perpendicular into the outside tunnel wall and into the earth-berm. A map of the expected dose rates for a vertical section through the earth-berm along the beam axis is presented in Fig. 5. The earth-berm extends up 8.5 meters with regard to the beam axis. Fig. 6 shows iso-contour lines of the dose rates on the surface of the earth-berm. Peak levels of dose rates of 1 rem/hr were found for this case. The figure indicates that radiation monitors outside of the tunnel system need to be placed within 10 meters of the beam impact point (coordinates origin) to be able to register elevated dose values above the trigger point of 20 mrem/hr.

Another scenario, the beam hitting any bulky accelerator component in the tunnel, was considered to be even more unlikely, than the previously discussed accident. In this case the dose levels on top of the earth-berm will be significantly higher compared to the previously mentioned case. In this case a field of secondary radiation is built up in the tunnel, which will have to penetrate only 5.7 meters of concrete and soil to reach the top of the earth-berm compared to the 8.5 meters from the first accident case. Hence, about 20 rem/hr are obtained in the hot spot on top of the earth-berm (see Fig. 7). Consequently, the area with doses exceeding the 20 mrem/hr level is with a radius of 16 meters somewhat larger as shown in Fig. 8 compared to the previous accident case.

V. EARTH-BERM EVALUATION FOR HIGH RADIATION AREAS

The soil thickness above all tunnel sections has been set to 5 meters anticipating line losses of maximum 1 W/m at 1GeV beam energy throughout the facility. In local areas, the line losses will exceed this maximum. The straight north section of the accumulator ring that houses three collimators capturing about 0.17% of the proton beam for beam cleanup during 2 MW operations will be with up to 20,000 Rem/hr the hottest radiation area in the tunnel system. Another hot spot will be the stripping foil in the injection section of the ring, which will capture 160 W unshielded. In these two areas the mitigation of the radiation by the earth-berm was evaluated.

The radiation transport calculations were performed using the MCNPX code applying detailed beam line and accelerator tunnel models. Constant sized particle populations were maintained throughout the earth-berm applying Russian roulette and splitting methods with geometrical importance zones. The calculations assumed 90%-compacted Tennessee soil with a density of 1.99 g/cc.

The dose rates on top of the earth-berm resulting from the calculations are plotted as color-coded maps in Fig. 9 and 10. In both cases, the hot spot of dose rates extends beyond the tunnel width. Peaks of dose rates of 0.4 mrem/hr and 7 mrem/hr were observed for the injection and collimation sections, respectively. All tunnel areas will be fenced and not accessible without authorization.

VI. HEATING OF BEAM DUMP AREAS

The SNS accelerator system includes three major beam dumps: a linac dump and an extraction dump for tuning purposes, each designed for 7.5 kW beam power, and the injection dump for capturing the H to proton beam conversion losses in the injection section of the accumulator ring, designed for 200 kW beam power. The energy deposition profiles in beam stops for a given beam power and at fixed proton energy depends not only on the beam profile, but also on the beam broadening effect of beam windows (location, material and thickness) upstream of the beam stop. Design iterations and changes in parameters triggered repeated recalculations of the nuclear heating profiles of these beam dumps. The present parameters are listed in Table I.

Table I: Parameters of beam stops and beam windows.

Dump Name	Power (kW)	Stop material	Window material	Window location
Linac	7.5	Steel	0.5 mm Inconel	12.4 m
Injection	200	Copper	2x1.6mm Alu	0.2 m
Extraction	7.5	Steel	0.5mm Inconel	16.8 m

The energy deposition characteristics were evaluated from full transport analyses of the window and beam stop configurations using beam profiles with characteristics as listed in Table II. Peak energy deposition, radial and axial half maximum values are presented in Table III for all beam stops.

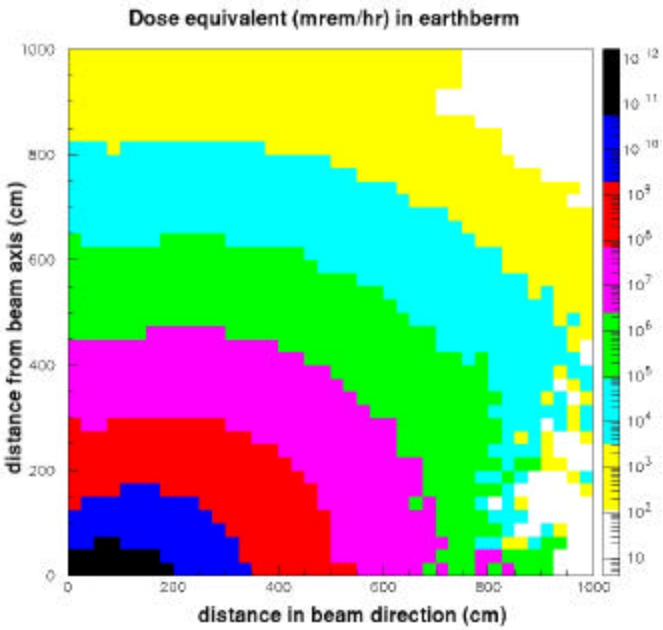

Fig. 5: Dose rate contours in the earth-berm for the case having the proton beam hitting the tunnel concrete wall and the earth-berm. The origin defines the beam intersecting the concrete wall. The earth-berm reaches up to the y level of 8.5 m.

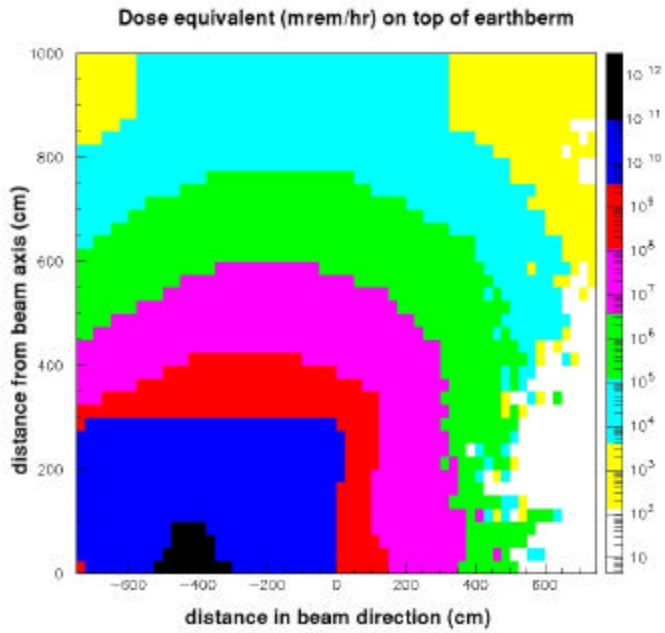

Fig. 7: Dose rate contours in the earth-berm for the case having the proton beam hitting a linac-to-ring dipole. The origin is defined by the proton beam axis intersecting the concrete wall. The earth-berm reaches up to the y level of 8.5 m.

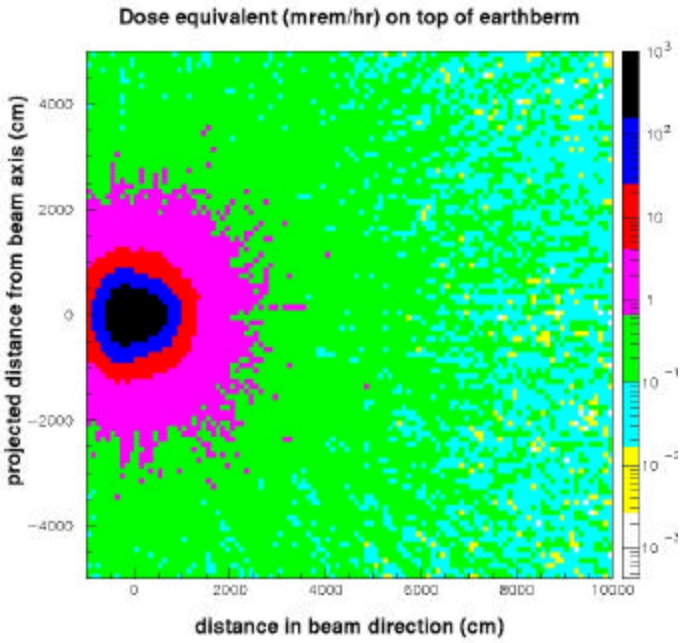

Fig. 6: Dose rate contours on top of the earth-berm averaged in a 2-meter-strong air layer for the case having the proton beam hitting the tunnel concrete wall and the earth-berm. The origin is the beam intersection point with the concrete wall projected on top of the earth-berm

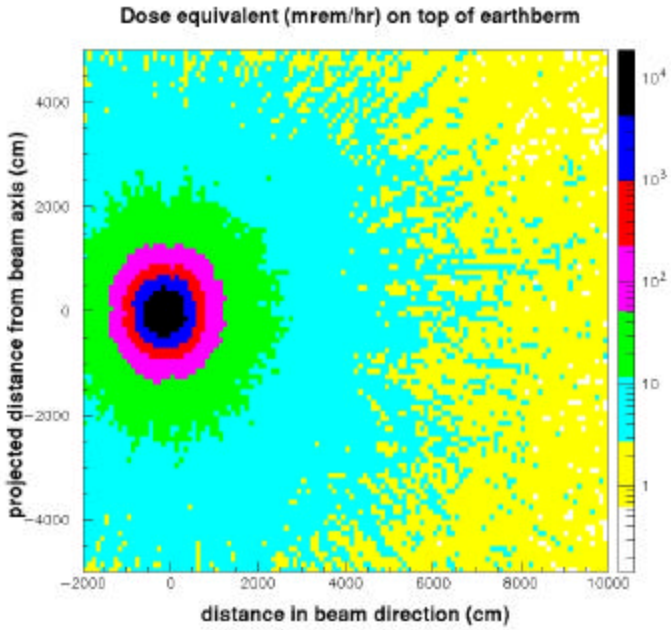

Fig. 8: Dose rate contours on top of the earth-berm averaged in a 2-meter-strong air layer for the case having the proton beam hitting a linac-to-ring dipole. The origin is the beam intersection point with the concrete wall projected on top of the earth-berm.

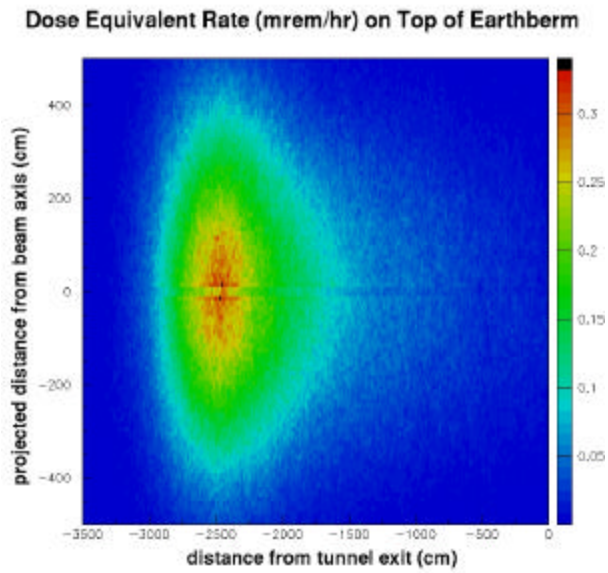

Fig. 9: Map of dose rates during operation on top of the earth-berm in the injection section of the accumulator ring.

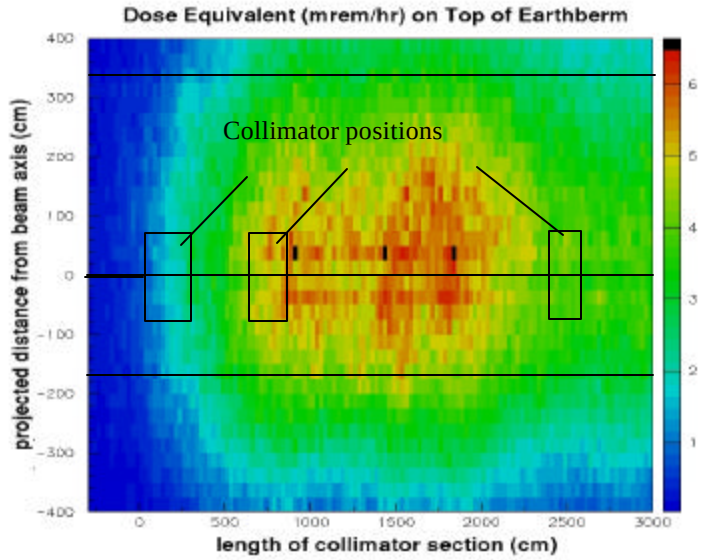

Fig. 10: Map of dose rates during operation on top of the earth-berm in the collimator section of the accumulator ring.

If the window thickness is increased to 2 mm the peak heating drops about a factor 3.7 and 1.5 for the linac and extraction dumps, respectively. A narrow profile of the incident beam, as for the linac beam dump, makes the heating rate profiles much more sensitive to an increase of the window thickness, compared to the wide beam.

Table II: Incident beam characteristics at the beam windows.

Dump Name	Power (kW)	Peak proton current (A/m^2)	FWHM of proton current (cm)
Linac	7.5	0.022	0.8
Injection	200	0.027	5
Extraction	7.5	0.001	6

Table III: Energy deposition characteristics in beam stops.

Dump Name	Power (kW)	Peak heating (W/cc)	Radial half max (cm)	Axial half max. (cm)
Linac	7.5	5.5	3	16
Injection	200	70	5	20
Extraction	7.5	0.8	8	19

VII. WATER ACTIVATION IN LINAC TUNNEL

In the linac tunnel, water is used for two reasons: firstly, for cooling the drift tube linac (DTL) and coupled cavity linac (CCL) structures, and secondly, for fire protection in a sprinkler water system. Radiation fields of up to 100 rem/hr, mainly from neutrons, will be generated in the linac tunnel by the interaction of H beam losses with structural materials during normal operations. The local fields in the linac structures are even higher. As a consequence, the water supplies become activated and need to be handled properly. The build up of the water activation was investigated to allow for waste water planning, and possible accident preparation.

The activation analyses are performed generally in two steps. Isotope production cross sections, which are used with neutron fluxes, are readily available up to 20 MeV of neutron energy[12]. For energies above and for particles other than neutrons, physics models predict directly isotope production rates. Both methods are used by extracting information from transport analyses applying the MCNPX code. Neutron fluxes and isotope production rates are fed into the ORNL activation analyses sequence (AAS)[13]. The AAS applies the ORIHET95 code that performs the buildup/decay calculations.

The radiation fields in the accelerator tunnel were calculated using a full scale linac model with detailed water cooling zones in the DTL and CCL. Although the

neutron fluxes were predicted to a satisfactory accuracy, the prediction of the high energy isotope production lacked behind for statistical reasons. Hence simple spherical water models were created, and exposed to selected neutron source spectra above 20 MeV to obtain improved high energy isotope production rates for the activation analyses. The resulting nuclide activities in the hottest DTL and CCL areas with half-lives longer than 1 minute are listed in Table IV assuming 6500 hours of operations. Corrosion products solved in water were not considered in the analyses. The activity in the sprinkler lines were found to be of the same magnitude on a per unit volume basis.

Table IV: Nuclide buildup in cooling loops of DTL and CCL after 6500 hours of operation at 2MW beam power.

Isotope	Half-life	Activities	
		CCL cavity cooling (Ci/cm^3)	DTL drift tube cooling (Ci/cm^3)
H 3	12.3y	3.81E-10	1.65E-10
BE 7	53d	9.53E-10	1.80E-10
BE 10	1.51e+6y	2.50E-16	3.49E-17
C 11	20min	3.64E-09	1.13E-09
C 14	5730y	7.85E-13	2.96E-13
N 13	10min	8.43E-10	1.90E-10
O 14	1.2 min	1.09E-10	2.12E-11
O 15	2.1 min	1.15E-08	4.49E-09

In a similar way the water activation of the three collimators located in the accumulator ring and a beam stop of similar design in the linac-to-ring transfer line were estimated. The first, second and third collimator in the ring scrape and capture 0.085, 0.042 and 0.046 % of the beam, respectively, the beam stop captures about 0.1%. The calculations were performed for 2 MW beam power. The nuclide activity presented in Table V was calculated for the arc beam stop for 30 years of operation at 5000 hours per year. The activity of the ring collimators scale with the beam power they capture.

Table V. Water activation in the arc beam stop after 30 years of irradiation.

Isotope	Half-life	Activity (Ci/cm^3)
H 3	12.3y	3.09E-4
BE 7	53d	5.36E-5
BE 10	1.51e+6y	2.29E-10
C 11	20min	9.54E-5
C 14	5730y	2.29E-10
N 13	10min	3.76E-5
O 14	1.2 min	1.47E-5
O 15	2.1 min	3.62E-4

VIII. OUTLOOK

The focus of the SNS accelerator shielding effort is to provide design solutions for the high-intensity beam facility that meet the ALARA principle to a minimum of cost. The work presented here covers many aspects of accelerator systems neutronics and evolved from many iterations of calculations and a huge amount of spent CPU time. And there is still work to be done, mainly for the accumulator ring and ring-to-target transfer line design, in preparation of the accelerator readiness reviews and for commissioning.

REFERENCES

1. National Spallation Neutron Source Conceptual Design Report, Oak Ridge National Laboratory, NSNS/CDR-2/VI, 1997.
2. R. L. Kustom, "An overview of the Spallation Neutron Source Project", Proceedings of the XX International Linac Conference, Monterey, August 21-25 2000.
3. F. X. Gallmeier and D. Raparia, 'Proton Beam Profiles at the target and at the Beam Dumps of the SNS', Fourth International Topical Meeting on Nuclear Applications of Accelerator Technology, American Nuclear Society, Washington D.C. (November 12-15, 2000).
4. Franz X. Gallmeier, "Shielding the SNS Klystron Building from the Linac," Fourth International Topical Meeting on Nuclear Applications of Accelerator Technology, American Nuclear Society, Washington D.C. (November 12-15, 2000).
5. Popova and J. Bucholz, 'Shielding and Activation Analyses for SNS 200 kW Ring Injection Beam Dump, Title I Design', Fourth International Topical Meeting on Nuclear Applications of Accelerator Technology, American Nuclear Society, Washington D.C. (November 12-15, 2000).
6. F. X. Gallmeier, "Calculations of operational and residual doses for the SNS linac", Fifth International Topical Meeting on Nuclear Applications of Accelerator Technology, American Nuclear Society, Reno, November 2001.
7. J. A. Bucholz, F. X. Gallmeier, I. Popova, 'Egress Shielding Studies for the SNS Accelerator System', Fifth International Topical Meeting on Nuclear Applications of Accelerator Technology, American Nuclear Society, Reno, November 2001.
8. F. X. Gallmeier, 'Radiation Transport through Complex Shield Penetrations in Accelerator Environments', Radiation Protection and Shielding Division 12th Biennal Topical Meeting, American Nuclear Society, Santa Fe, New Mexico (April 14-18, 2002).

9. H.G. Hughes et al., "MCNPX for Neutron-Proton Transport," International Conference on Mathematics & Computation, Reactor Physics & Environmental Analysis in Nuclear Applications, American Nuclear Society, Madrid, Spain, September 27-30, 1999.
10. N. Catlan-Lasheras et. al., "*Accelerator physics model of expected beam losses along the SNS accelerator facility during normal operation*", ANA/AP Technical Note 07, UT-Battelle, LLC, Oak Ridge (March, 2001).
11. Irina Popova,, 'Comparison of Discrete Ordinates and Monte Carlo Methods for designing an Steel Shielding Door', in this proceedings.
12. B. Pashchenko and P. K. McLaughlin, "FENDL/A-1.1, Neutron Activation Cross Section Data Library for Fusion Applications," IAEA-NDS-148, Rev. 2 (1995).
13. N. Odano et al., "Development of the Activation Analysis Calculational Methodology for the Spallation Neutron Source (SNS)," 1998 ANS radiation Protection and Shielding Division Topical Conference, American Nuclear Society, Nashville, Tennessee, April 19-23, 1998; and Greg McNeilly, "AAS-Activation Analysis System", SNS-101040200-TR0003R00, UT-Battelle (1999).